INFRARED THERMAL-WAVE STUDIES OF COATED SURFACES

T. Ahmed, P.K. Kuo, L.D. Favro, H.J. Jin, P. Chen, and R.L. Thomas

Department of Physics and Institute for Manufacturing Research
Wayne State University
Detroit, MI 48202

INTRODUCTION

In recent years plasma-sprayed coatings and polymer coatings have found wide application in manufacturing. Although the quality of the coatings improved over the years, there is a need for reliable NDE techniques to assess the quality and test the integrity of these coatings. Most existing techniques are not suitable for real-time applications. The introduction of synchronous thermal wave video imaging techniques using infrared cameras[1, 2] has made it possible to make images of thermal wave phenomena in almost real-time. In this work we describe the application of a pulsed heating and synchronous infrared thermal wave detection technique to image sub-surface defects in plasma-sprayed thermal barrier coatings and polymer coatings on metal substrates.

EXPERIMENTAL SET-UP

The experimental technique used in this study is the box-car infrared video technique [3,4] which was introduced in the 1988 QNDE conference. This technique uses a commercial infrared video camera (Inframetrics IR600), coupled to a real-time dedicated image processing system (DataCube), and a computer workstation (Sun 3/160C) to do pixel by pixel image processing and averaging in synchronism with the heat source. In this technique the camera is used as a box-car integrator for repetitive pulse heating of the sample. A block diagram of the imaging system is given in Fig. 1. The heat source consists of two 5kJ flashlamps with 5 ms pulse duration. The image processing involves accumulation of an image in a given time gate after a fixed delay from the heating pulse. A gate consists of a frame, or several frames in succession, grabbed at some specified time after a given heating pulse. Up to four independent gates may be set within *each* heating pulse cycle. Each of the resulting four images is combined with images taken with previous heating pulses to form four averaged images in four separate frame buffers. After a suitable number of averages with a given set of gates, the averaged images are transferred to a computer workstation (Sun 3/160) which, by appropriate arithmetical manipulation of the images, is able to remove background effects and thermal emissivity artifacts. The combination of this post-processing in the computer with the prior, real-time averaging in the image processor, improves the sensitivity of the camera and allows the imaging of defects which are ordinarily invisible to the camera.

The maximum thermal image contrast for a particular sample depends on the thermal properties of the material, its thickness and the incident heat pulse duration and power. Therefore, when imaging a new material or combination of materials, one must first determine the appropriate time scale(s) for setting the box-car gates. This is accomplished by analyzing preliminary images with our (WSU-developed) system software. This software includes provisions for mouse-driven, on-screen plotting of the time dependence of the

Review of Progress in Quantitative Nondestructive Evaluation, Vol. 9
Edited by D.O. Thompson and D.E. Chimenti
Plenum Press, New York, 1990

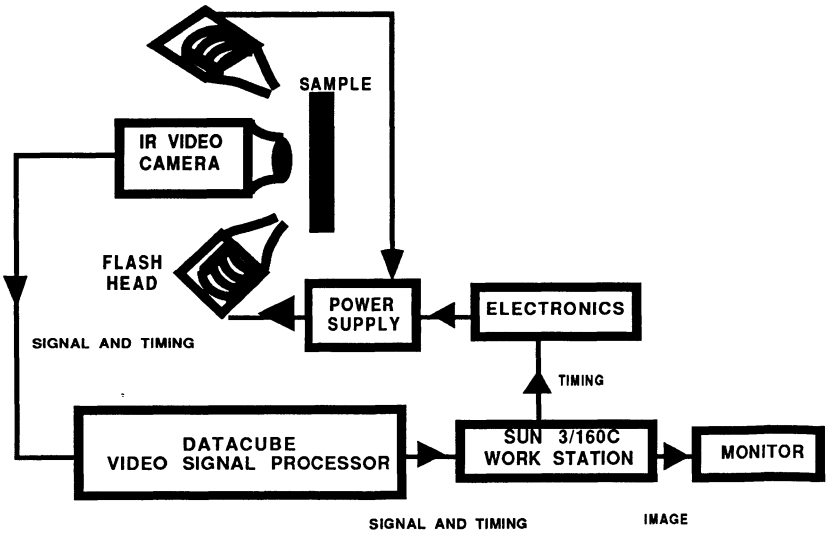

Figure 1. Block diagram of the thermal wave video imaging system (Box-car scheme).

spatial average of the signals corresponding to any arbitrary rectangular area of the image, and for comparing the time dependences for different areas. This comparison is used to set gate delays and gate widths which maximize the thermal wave contrast of the image. This process takes only a few minutes and then the system is set to produce the final image of the sample. Subsequent samples of the same type require no further set-up, and are done essentially in real time. The ability to plot the time dependence of the average temperature of arbitrary regions of the sample also provides a powerful materials characterization capability through the comparison of the experimental curves with theoretical calculations with different models of the subsurface structure.

IMAGE PROCESSING

The real-time image processing system was built using DataCube Inc. hardware and WSU designed software running on a Sun 3/160C color workstation. The video image acquisition is shown schematically in Fig. 2. It consists of a video acquisition and display module, a digital video storage module and a general purpose processing module. The input RS-170 analog video signal is sent to the video acquisition module which contains a phase-locked loop (not shown) which takes the timing information from the sync stripper and derives master timing signals from it. These timing signals synchronize all boards in the system. The remaining analog video signal is filtered and amplified or reduced using the gain and offset controls, before it is sent to an 8 bit A/D converter. The resulting digitized video signal is a 10 MHz stream of scan-sequential data. These data can be modified by the input look-up table (LUT) and fed to the processing module. In the processing module, the data is modified using the LUT, and is put out as a 16-bit signal. This signal is combined with the 16-bit data previously accumulated in the storage module, using the arithmetic logic module (ALU). The signal from the ALU is sent back to the storage module, replacing the previously accumulated data, and the whole process is repeated until a predetermined number of averages have been carried out.

Each storage module is capable of holding three (512x512) frames of 8-bit deep digital video signal. The 8-bit image data are stored in two image buffers (high byte and low byte) to retain the 16-bit accuracy. The system is capable of processing the 10 MHz data stream, while retaining its full 16-bit accuracy. It can perform temporal and spatial filtering, image merging, image subtraction and addition, and/or other simple arithmetic operations in real-time.

The processed images are transferred to the color workstation that is used for controlling the video data acquisition for subsequent post-processing, storage and display. The image data that are transferred to the color workstation are in the 8-bit format. These data are obtained from the 16-bit image data by selecting an 8-bit image window with optimum contrast, but without overflow of the data. The image display is accomplished using a WSU-developed custom colormap software system. The colormap composition is fully interactive and mouse driven, using the facilities of the window system in the workstation

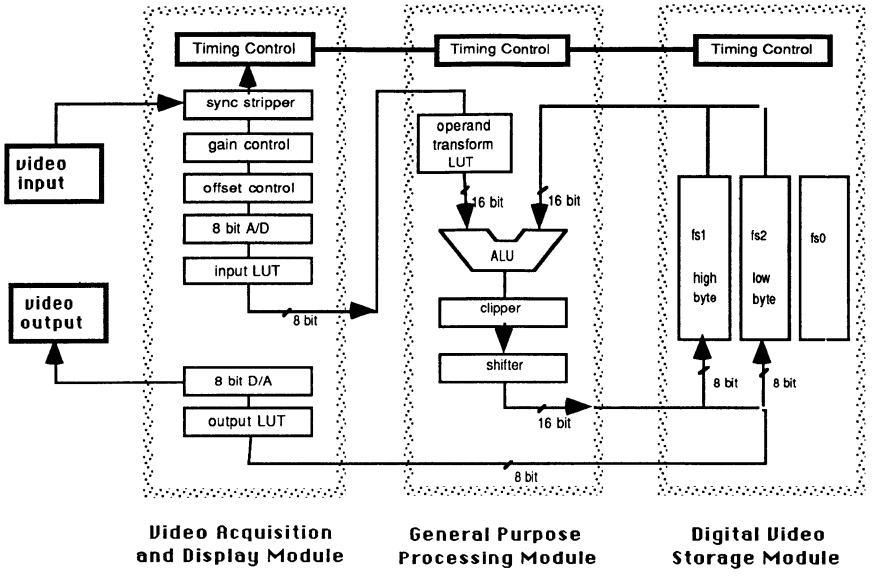

Figure 2. A schematic diagram of the video image processing architecture.

RESULTS AND DISCUSSION

As mentioned in earlier discussion, the preliminary analysis of a sample is accomplished by comparing the time dependence of the surface temperature for different areas of the sample. This comparison is then used to determine the gate delays and gate widths at which the thermal wave contrast of the image is maximum. To illustrate this procedure, a zoomed optical image of a thermal barrier coating is shown in Fig.3 where the two rectangular boxes on the image show the areas of the spatial averages. The box on the left is over a subsurface crack and the one on the right is on a good region. Fig. 4 shows the temperature/square-root-time dependence of these two regions as displayed by our real-time system. From the data it is evident that the subsurface crack impairs conduction since the region over the crack cools more slowly.

An illustrative example of full field box-car imaging is given in Fig. 5. Here, we show a box-car thermal wave image of a thermal barrier coating on a thick (1") Al-alloy plate. The image shows regions of delamination (darker, flower-petal shaped pattern) produced during a simulated combustion engine test.

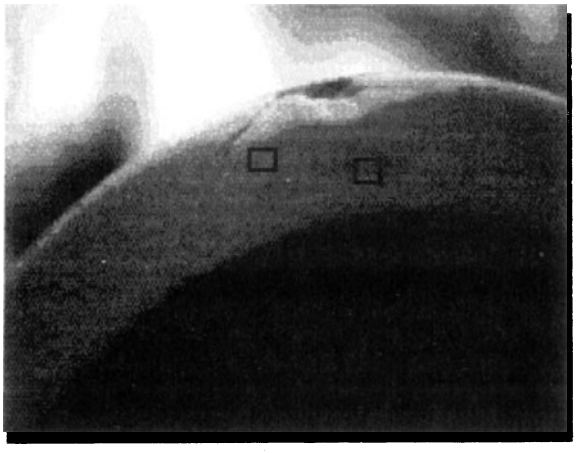

Figure 3. Zoomed optical image of a thermal barrier coating with defects.

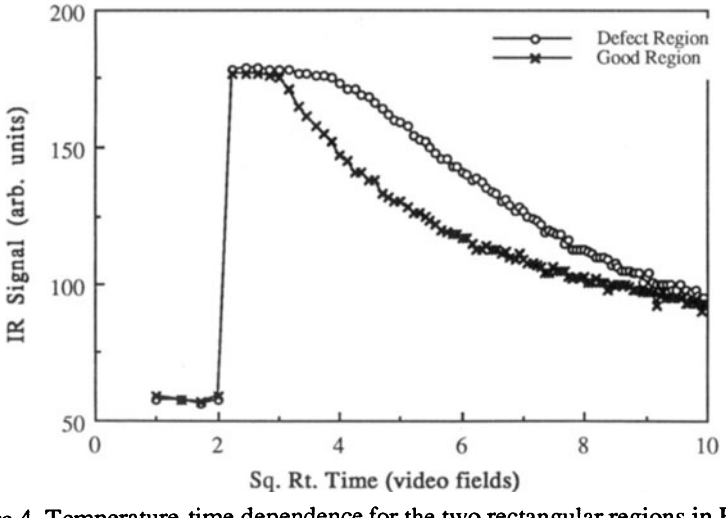

Figure 4. Temperature-time dependence for the two rectangular regions in Fig.3.

A next set of illustrative examples are of multilayered plasma-sprayed thermal barrier coating on top of iron pistons from an internal combustion engine. The first image (Fig.6) shows a box-car image of a defective coating showing delaminations (dark areas on top and bottom of the image) produced during the sample preparation stage. The second image (Fig.7) is one of another piston, which shows no defects at this stage, before it was installed in an engine. Finally in Fig.8, we show a box-car image of the same piston as in Fig.7 after the engine had been run steadily for several weeks. The most obvious change between the "before" and "after" images is the large region on the upper right of the rim in which the coating has spalled off. Of more interest are the "hot spots" (dark regions) at the center and at various points around the rim. As demonstrated by subsequent sectioning of the sample, these represent regions in which the bonding of the coating to the substrate has failed, but for which spalling has not yet occurred.

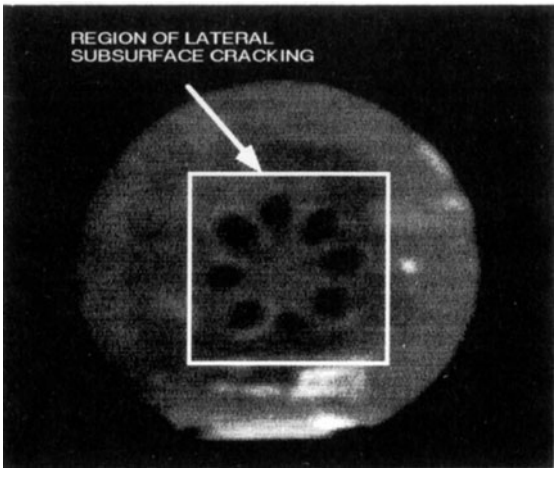

Figure 5. A full-field box-car thermal wave image of a thermal barrier coating on Al-alloy substrate showing regions of delamination.

The final pair of illustrative examples, shown in Figs. 9 and 10, demonstrates the application of our box-car infrared thermal wave imaging technique to image sub-surface defects in automotive coatings. These samples are polymer coatings on steel substrates. Fig.9 shows an optical image of one of the coating samples on which artificial defects were created by the scratch and tape-pull method. The region of interest on this optical image is the region around the three vertical lines near the center of the image. These scratches have significantly different depths with the depth increasing to the right. A close-up (zoomed) thermal wave image of that region is shown in Fig.10. Although the three vertical lines are visible in the optical image (Fig.9), in the thermal wave image (Fig.10) only the two lines on the right are visible. The scratch on the left is apparently too superficial to affect the thermal wave signal. The line in the center of Fig.10 is dark, indicating that the coating is broken, thus exposing the low-emissivity metal underneath. The hot or the bright line on the right represents a region adjacent to the scratch in which the bonding of the coating to the substrate has failed.

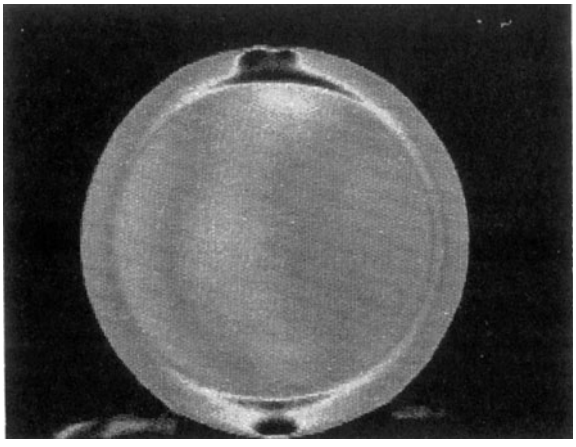

Figure 6. A box-car thermal wave image of a defective coating showing delaminations.

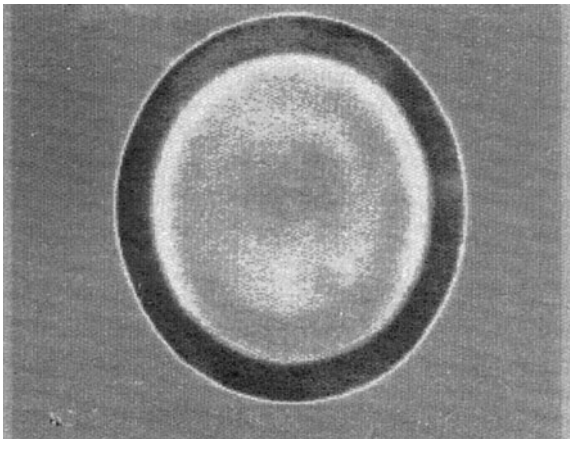

Figure 7. A box-car thermal wave image of a thermal barrier coated piston before it was installed in the engine.

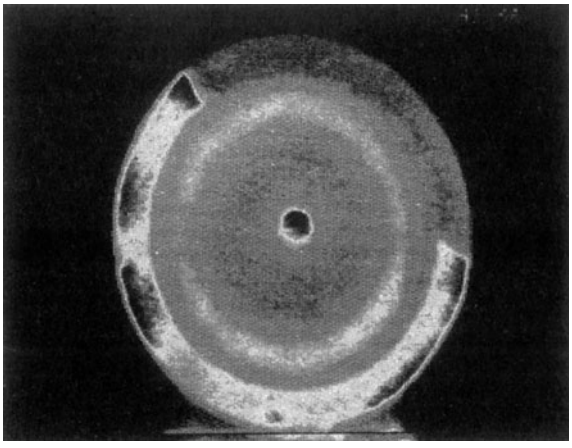

Figure 8. A box-car thermal wave image of the piston in Fig.7 after the engine had been run for several weeks.

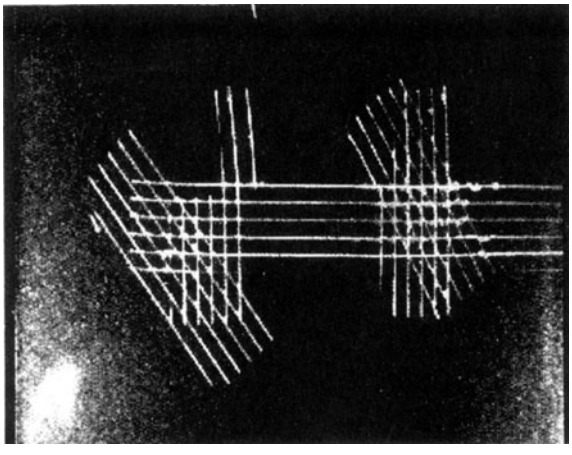

Figure 9. An optical image of an automotive coating with artificial defects created by scratch and tape-pull method.

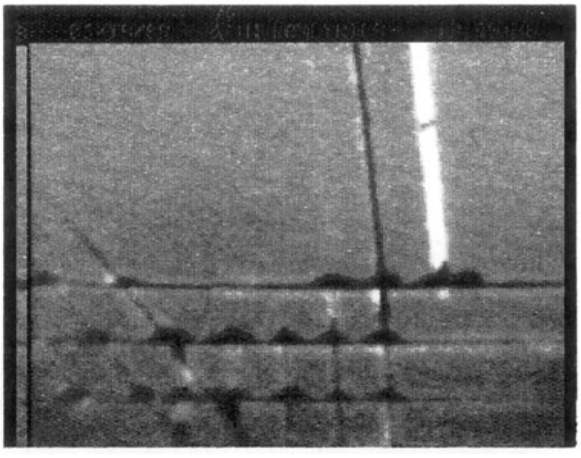

Figure 10. A close-up (zoomed) box-car thermal wave image of the automotive coating in Fig.9.

CONCLUSIONS

In this work we have described a thermal wave infrared video imaging technique in which a infrared video camera is used as a box-car integrator for pulsed thermal wave images. By using synchronized heating and detection, together with image averaging methods, we have made substantial improvements in signal-to-noise ratio of the camera.

ACKNOWLEDGMENTS

This work was sponsored by the Center for Advanced Nondestructive Evaluation, operated by Ames Laboratory, USDOE, for the Air Force Wright Aeronautical Laboratories under contract No. W-7405-ENG-82 with Iowa State University, by the Ford Motor Company, and by the Institute for Manufacturing Research, Wayne State University.

REFERENCES

1. See for example, W.N. Reynolds, Can. J. Phys. **64**, 1150 (1986)
2. P.K. Kuo, Z.J. Feng, T. Ahmed, L.D. Favro, R.L. Thomas, and J. Hartikainen, in Photoacoustic and Photothermal Phenomena, P. Hess and J. Pelzl, Eds., Springer-Verlag, 415 (1988)
3. P.K. Kuo, T. Ahmed, H.J. Jin, L.D. Favro, R.L. Thomas, J. Hartikainen and J .Jaarinen, Review of Progress in Quantitative Nondestructive Evaluation, D.O. Thompson and D.E. Chimenti, Eds., Plenum Press, Vol.**8**, 1305-1310, 1989
4. T. Ahmed, P.K. Kuo,H.J. Jin, L.D. Favro, R.L. Thomas, Review of Progress in Quantitative Nondestructive Evaluation, D.O. Thompson and D.E. Chimenti, Eds., Plenum Press, Vol.**8**, 1385-1392, 1989